Potential-field interpretation of the Capricorn Orogen, Western Australia: worms, forward modelling, and 3D inversion

by

JA Goodwin[1]

Introduction

The deep seismic lines 10GA–CP1, 10GA–CP2, and 10GA–CP3, collected across the Capricorn Orogen by AuScope, the Geological Survey of Western Australia (GSWA), and Geoscience Australia (GA) (Kennett et al., 2011), extend from the Pilbara Craton in the north, across the Capricorn Orogen, to the Yilgarn Craton in the south. The aim of these seismic lines was to provide insight into the geological structure of the Capricorn Orogen, and to explore its relationship with the Pilbara and Yilgarn Cratons. To further aid interpretation, and to add value to the seismic data, an analysis of the potential-field data (gravity and magnetics) was also undertaken using a range of geophysical data analysis techniques. These consist of: multiscale edge detection (worms), forward modelling, and 3D inversion. By applying all three analysis techniques to the potential-field data, a number of geophysical terranes, major trends, and contrasting properties relating to the subsurface geology have been identified, allowing for a detailed comparison with the seismic interpretations provided by Thorne et al. (2011) and Johnson et al. (2011).

Interpretation techniques

All interpretation techniques were performed on gravity data extracted from the 3rd edition of the Gravity Anomaly Map of Australia (Bacchin et al., 2008), and on magnetic data extracted from the 5th edition of the Magnetic Anomaly Map of Australia (Milligan et al., 2010), with a variable reduction to the pole (RTP) applied.

Multiscale edge detection (worms)

Multiscale edge detection is a technique used to highlight areas of contrast in potential-field data (Archibald et al., 1999). These areas of contrast are represented as edges, referred to as worms, which are generated across a range of levels of upward continuation. When viewed together, the worms form 3D surfaces whose shapes and orientations are related to contrasting properties in the subsurface geology. Property contrasts in potential-field data are often the result of discontinuities or interfaces where contrasting rock materials occur, such as at faults, unconformities, or intrusive contacts.

Worms were generated for the Capricorn Orogen data using the multiscale edge detection function in Intrepid software (version 4.2.3). For both gravity and magnetic grids, 12 upward continuation levels, with each level varying by a factor of 1.4, were specified using the Canny points calculation method. A variable reduction to the pole (RTP) was applied to the magnetic grid before multiscale edge detection was undertaken. Features in the worms were delineated following the methods of Archibald et al. (1999) and Holden et al. (2000), who infer that higher continuation levels correspond to features at relatively greater depths, and that worm orientations relate to the orientation of contacts.

2.5D Forward modelling

2.5D forward modelling was carried out to test the validity of the interpreted seismic sections in relation to the magnetic and gravity data. 2.5D modelling is the process of modelling two-dimensional bodies in a three-dimensional space, by extending the strike length of a body to a distance that is large enough, perpendicular to the section, to avoid edge effects. Rock properties (density and magnetic susceptibility) are added to the interpreted bodies, and the modelled magnetic and gravity response is then compared to the observed response. A good fit between the modelled and observed indicates that the interpreted seismic sections are consistent with the magnetic and gravity data.

Gravity and magnetic data were extracted along the seismic line traverses using the dataset resampler tool in Intrepid. 2.5D forward models were then created using ModelVision v11.0 software, extending from 600 m above to 60 km below the datum. To better approximate the 3D nature of the bodies in a 2D environment, the models

1 Minerals and Natural Hazards Division, Geoscience Australia, GPO Box 378, Canberra ACT 2601.

were extended 120 km in strike length (60 km on either side of the line) and 60 km beyond the ends of the seismic line to avoid edge effects. For both gravity and magnetic data, an initial model was produced where the geometries identified in the seismic interpretation were used to constrain the architecture, and only the rock properties (density and magnetic susceptibility) were adjusted to achieve a fit with the observed data. A modified model was also produced, with both geometry and rock properties adjusted to achieve a fit. Rock property data from Emerson (1990), Telford et al. (1990), and Clark and Emerson (1991) were used as guides to assign density and magnetic susceptibility values. The effects of remnant magnetization were ignored as they are generally considered a minor component of the observed signal. The scales shown on the forward models are in kilometres, and assume that one second of two-way travel time (TWT) is equal to three kilometres depth (based on an average crustal velocity of 6000 m/s).

3D inversion

Inversion is a mathematical process used for acquiring a set of parameters that both describe a model and are consistent with a set of observations. In this case, the observations are the gravity and magnetic data, and the parameters describing the model are density and magnetic susceptibility, respectively.

3D inversions were performed with the University of British Columbia – Geophysical Inversion Facility's (UBC–GIF) inversion software — particularly the GRAV3D (version 3) and MAG3D (version 4) program libraries. The gravity and magnetic inversion methods outlined by Li and Oldenburg (1996, 1998) were used; however, the process of model-based trend removal has only been undertaken for the gravity data, not for the magnetic data. Inversions were performed at the National Computational Infrastructure (NCI) supercomputer facility (hosted by the Australian National University) with parallelized UBC–GIF software. For the magnetic inversions, a Curie Depth of 32 km was determined (assuming a Curie Temperature of 580°C), using a thermal conductivity estimate of 2.5 W/mK (Beardsmore and Cull, 2001, fig. 4.1.) and a heat flow of 45 mW/m^2 (Cull and Denham, 1979). Finally, the geothermal gradient was estimated at 18°C/km following the equation: Q (surface heat flow) = β (geothermal gradient) × λ (thermal conductivity). The inversions presented here are unconstrained and, as a result, they are not influenced by the seismic line interpretation or the surface geology. This also ensures that they are free from user bias.

Geophysical interpretation

Seismic line 10GA–CP1

The northern end of seismic line 10GA–CP1 is dominated by high-amplitude, short-wavelength magnetic anomalies, and high-amplitude gravity anomalies, both associated with banded iron-formations of the Hamersley Group (Fig. 1a,b). The Hamersley Group outcrops along the seismic line at the Turner Syncline, which is flanked on either side by a smooth textured, magnetic low correlating with the basalt-dominated Fortescue Group (Fig. 1a,c). Overprinting areas of the Fortescue Group are magnetic haloes, such as those seen between approximately CDPs 4100 and 5300, which correspond to the folded and faulted margins of the Rocklea Dome (Fig. 1a). Together, these features define a terrane separated from the southern end of the seismic line by the Nanjilgardy Fault.

A series of northwest-trending lineaments, observed in the magnetic data at the southern end of the seismic line, can be seen to overprint a broad wavelength, ovoid magnetic high (Fig. 1a). These lineaments are continuous, and can be traced northwest to outcrops of Leake Spring Metamorphics (Fig. 1a,c), which are inferred to be a correlative of the upper Wyloo Group (Cawood and Tyler, 2004; Sheppard et al., 2007). This interpretation is supported by the magnetic data, where irregularly shaped, high-amplitude anomalies coincide with outcrops of the Leake Spring Metamorphics before becoming increasingly linear, with lower amplitude responses, as they grade into the upper Wyloo Group to the southeast (Fig. 1a).

The Turner and Hardey Synclines, in the north of the study area, are visible in the both the gravity and magnetic worms, with upward continuation heights of 1400–28 930 m (Fig. 2). This suggests that the Hamersley Group is the dominant source of magnetic and gravity anomalies at the northern end of the seismic line. The large ovoid magnetic high identified in the magnetic data is delineated by magnetic worms in the south, with upward continuation levels of 14 760–56 703 m, which extend to outcrops of the Hamersley Group towards the northwest. The extension of these worms may indicate that this large ovoid magnetic high is related to the Hamersley Group. Approximately from CDPs 5500 to 6000, gravity worms, with upward continuation levels of 3842–56 703 m, define a southwest-dipping contact, possibly related to contrasting densities below the Fortescue Group, where south-dipping layers are observed in the seismic data (Thorne et al., 2011).

The Hamersley Group heavily influences both the 3D magnetic and gravity inversions, with a region of high magnetic susceptibility (≥0.1 SI) and high density (≥0.05 g/cm^3) occurring approximately between CDPs 3000 to 4000, and extending down to 15 km depth (Fig. 3). This body relates to the Turner Syncline, and has been forward modelled with a magnetic susceptibility of 0.20 – 0.40 SI and a thickness of approximately 2.5 km to match the seismic interpretation (Fig. 4; Thorne et al., 2011). As the effect of remnant magnetization in the Hamersley Group significantly increases the observed magnetic anomalies (Guo et al., 2011), only the shape of the wavelength has been matched by the forward model, not the amplitude.

Another region of high magnetic susceptibility (≥0.1 SI) and high density (≥0.05 g/cm^3) is observed between CDPs 6200 and 6800 in the magnetic inversion, and between CDPs 5500 and 6300 in the gravity inversion (Fig. 3). These anomalies are sourced from high density, high magnetic susceptibility rocks of the Hardey Syncline, which are located off the seismic line (see surface geology; Fig. 1c). As a result, this body has not been included in the forward modelling.

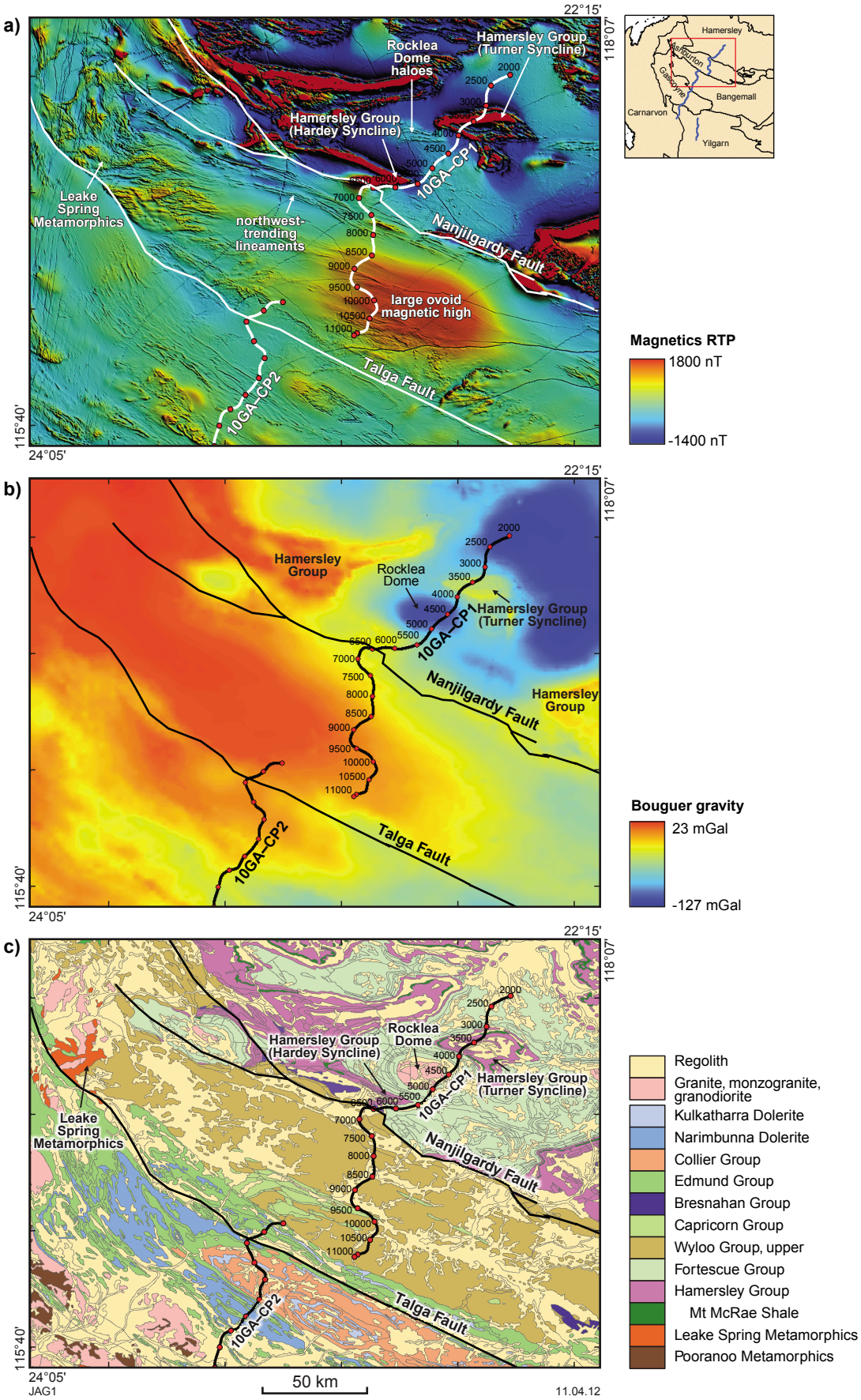

Figure 1. **a) Magnetic grid RTP (with values outside the 98th percentile removed, and sun shading from the northeast applied to highlight contrast in the data); b) bouguer gravity grid; c) 1:1 000 000 scale surface geology map covering seismic line 10GA–CP1.**

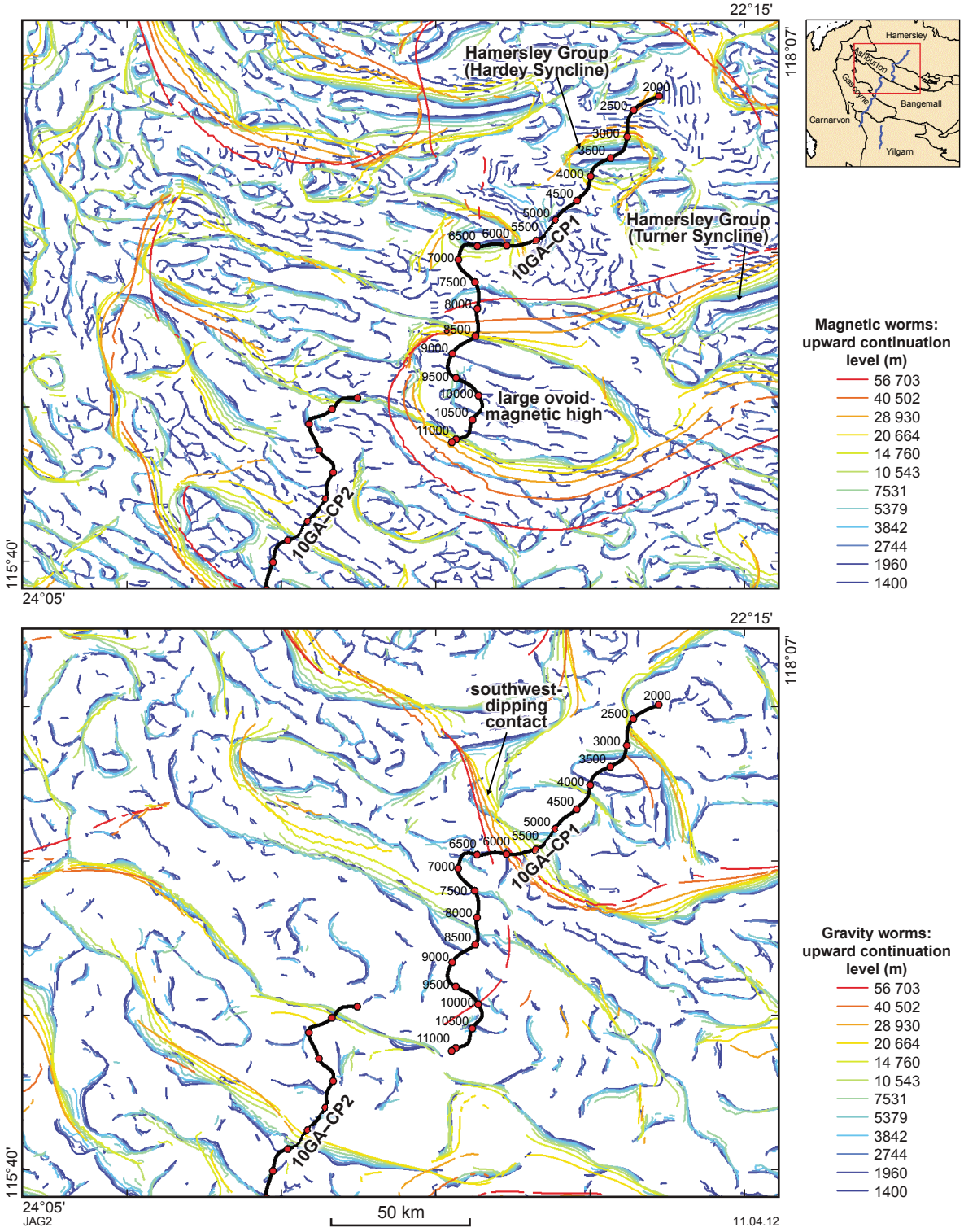

Figure 2. Worm images, covering seismic line 10GA–CP1, for magnetic (a) and gravity (b) data.

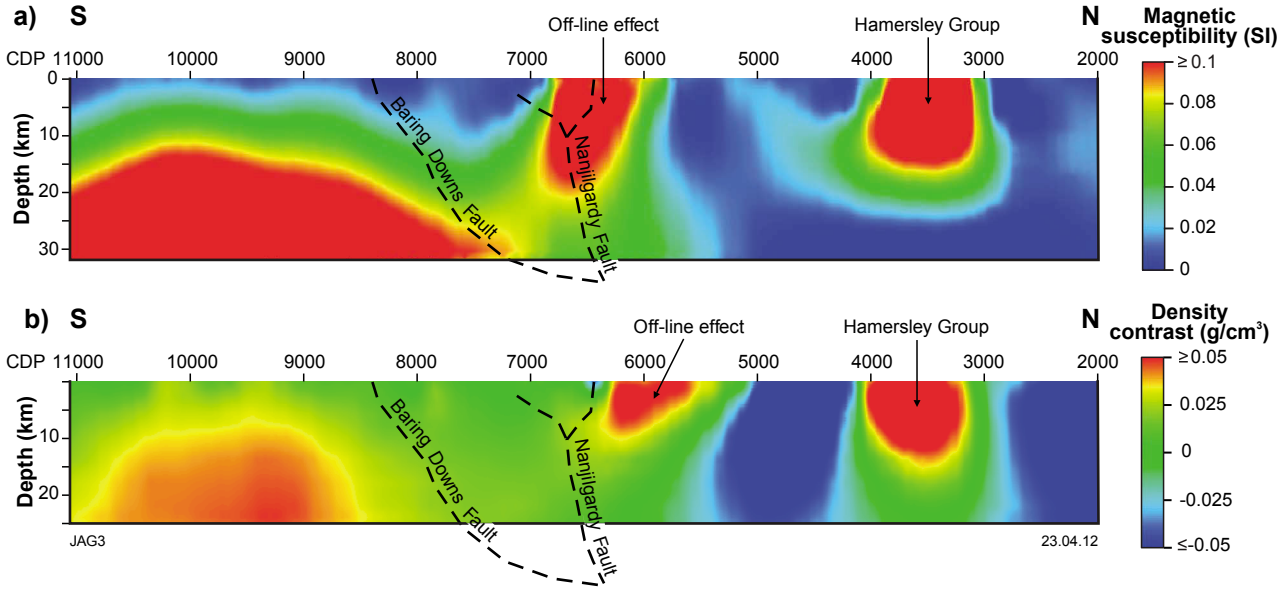

Figure 3. Inversion models extracted along seismic line 10GA–CP1: a) magnetic susceptibility model; b) density model.

At the southern end of seismic line 10GA–CP1, an upward doming body, ranging 12–25 km depth, and with a magnetic susceptibility of ≥0.1 SI, is observed in the magnetic inversion (Fig. 3). The northern margin of this magnetic body defines a north-dipping contact, consistent with the dip direction of the Baring Downs Fault, which itself is interpreted as a suture marking the southernmost extent of the granite–greenstone basement (Thorne et al., 2011). The gravity inversion also suggests that the Baring Downs Fault separates relatively denser units in the south from less dense units in the north (Fig. 3).

Two separate seismic interpretations have been suggested by Thorne et al. (2011) for seismic line 10GA–CP1, and these geometries have been used to create two different forward models — the initial interpretation (Fig. 4a) has a thicker Bandee Seismic Province, whereas the alternative interpretation (Fig. 4b) has the Hamersley and Fortescue Groups present above the Bandee Seismic Province (Fig. 4b). A third forward model, the modified interpretation, has also been created, in which the Hamersley Group in the south is closer to the surface than in the initial or alternative interpretations (Fig. 4c).

A regional gravity low, reaching −100 mGal, is observed at the northern end of the seismic line coinciding with the Pilbara Craton granite–greenstone terrane, and is forward modelled with densities of 2.60 – 2.72 g/cm^3 (Fig. 4). Nested within this gravity low is a broad-wavelength gravity high, reaching −43 mGal, associated with the overlying Hamersley Group (3.20 g/cm^3). The Hamersley Group itself has a short-wavelength gravity low nested within it, caused by a thin succession of the overlying Turee Creek Group (2.80 g/cm^3; Fig. 4).

Towards the southern end of seismic line 10GA–CP1, the regional gravity trend increases to −13 mGal, and this trend has been accounted for in the initial interpretation by attributing a density of 2.90 g/cm^3 to the Bandee Seismic Province (Fig. 4a). In both the alternative and modified interpretations (Fig. 4b,c), this increase in the gravity trend is accounted for by the Hamersley (3.20 g/cm^3) and Fortescue (2.90 g/cm^3) Groups. This increase in gravity also coincides with an increase in the regional magnetic trend, which peaks at 1250 nT in this area. This trend is accounted for by the Bandee Seismic Province (0.08 SI) in the initial interpretation, and by the Hamersley Group (0.10 – 0.20 SI) in the alternative and modified interpretations (Fig. 4). The regional magnetic high is best accounted for by the modified interpretation due to the upward doming geometry of the Hamersley Group (Fig. 4c). Of the three forward models presented here, the initial and modified models, seen in Figures 4a and 4c, respectively, show the best fit with the gravity and magnetic anomalies observed along the seismic line 10GA–CP1.

Seismic line 10GA–CP2

The Edmund Group covers the northern end of seismic line 10GA–CP2 and is intruded by sills of Narimbunna Dolerite (Cutten et al., 2011). These dolerite sills appear as northwest-trending undulations and cause short-wavelength magnetic anomalies throughout the extent of the Edmund Group (Fig. 5a). Mottled and irregular magnetic textures, associated with high-amplitude magnetic anomalies, are observed crossing the seismic line from CDPs 8000 to 8600 and from CDPs 9500 to 14000 (Fig. 5a), coinciding with outcrops of the Leake Spring Metamorphics (Fig. 5c). The Leake Spring Metamorphics are variably intruded and deformed by granites of the Moorarie and Durlacher Supersuites, which developed magnetic contact metamorphic aureoles. The bouguer gravity grid highlights high-amplitude anomalies

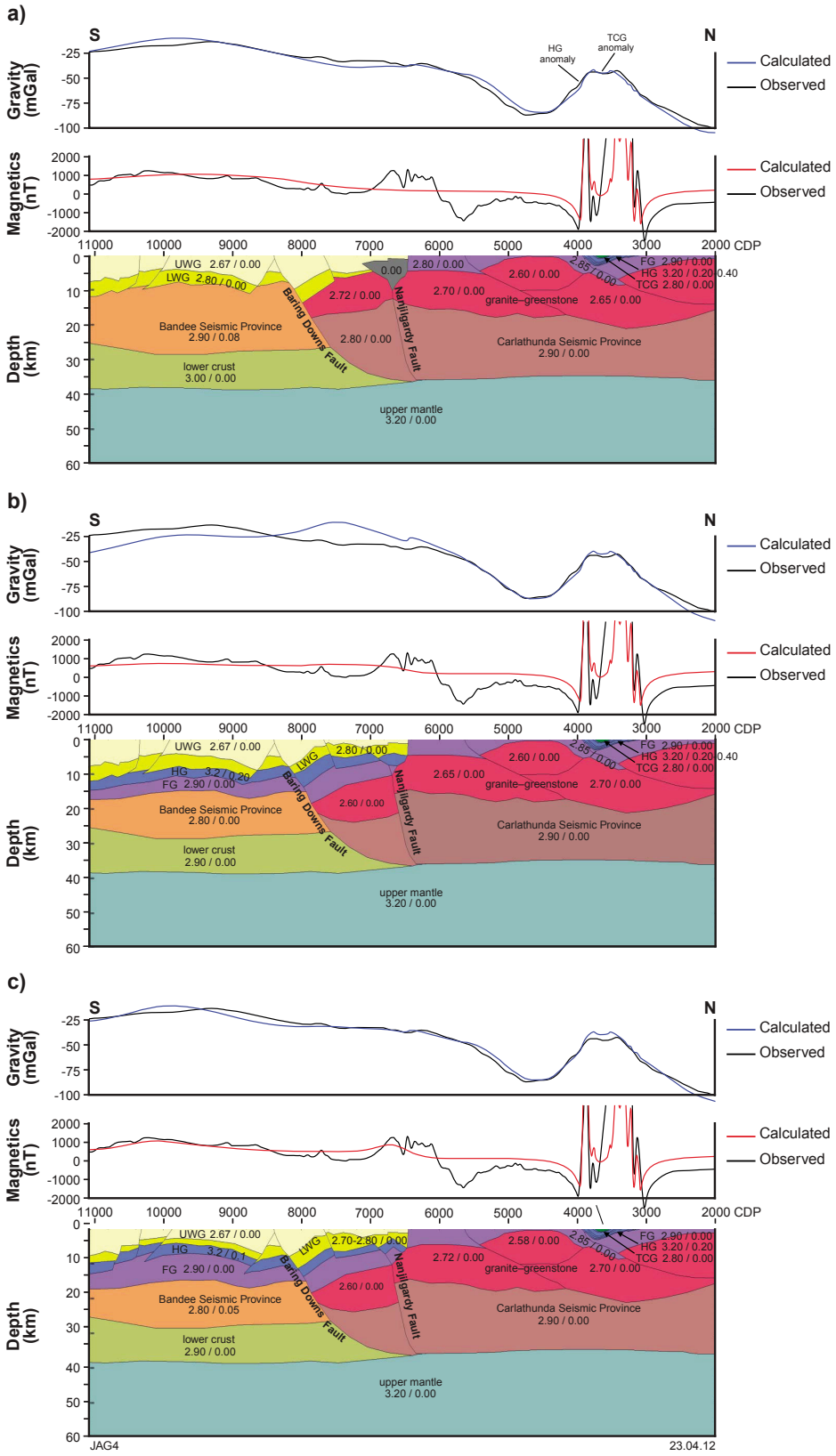

Figure 4. **Forward models for seismic line 10GA–CP1: a) initial interpretation using geometries described by Thorne et al. (2011); b) alternative interpretation using geometries described by Thorne et al. (2011); c) modified model, with the Hamersley Group in the south interpreted to be closer to the surface than in (b). Note that the outcropping Hamersley Group anomalies (between CDPs 3000 and 4000) exceed 5000 nT; to highlight variation in the southern section of the line, the scale for the observed magnetic profile was therefore set to a maximum of 3000 nT. Rock property values are listed on the figure as density (g/cm^3) / magnetic susceptibility (SI). Abbreviations used: FG — Fortescue Group; HG — Hamersley Group; TCG — Turee Creek Group; LWG — lower Wyloo Group; UWG — upper Wyloo Group.**

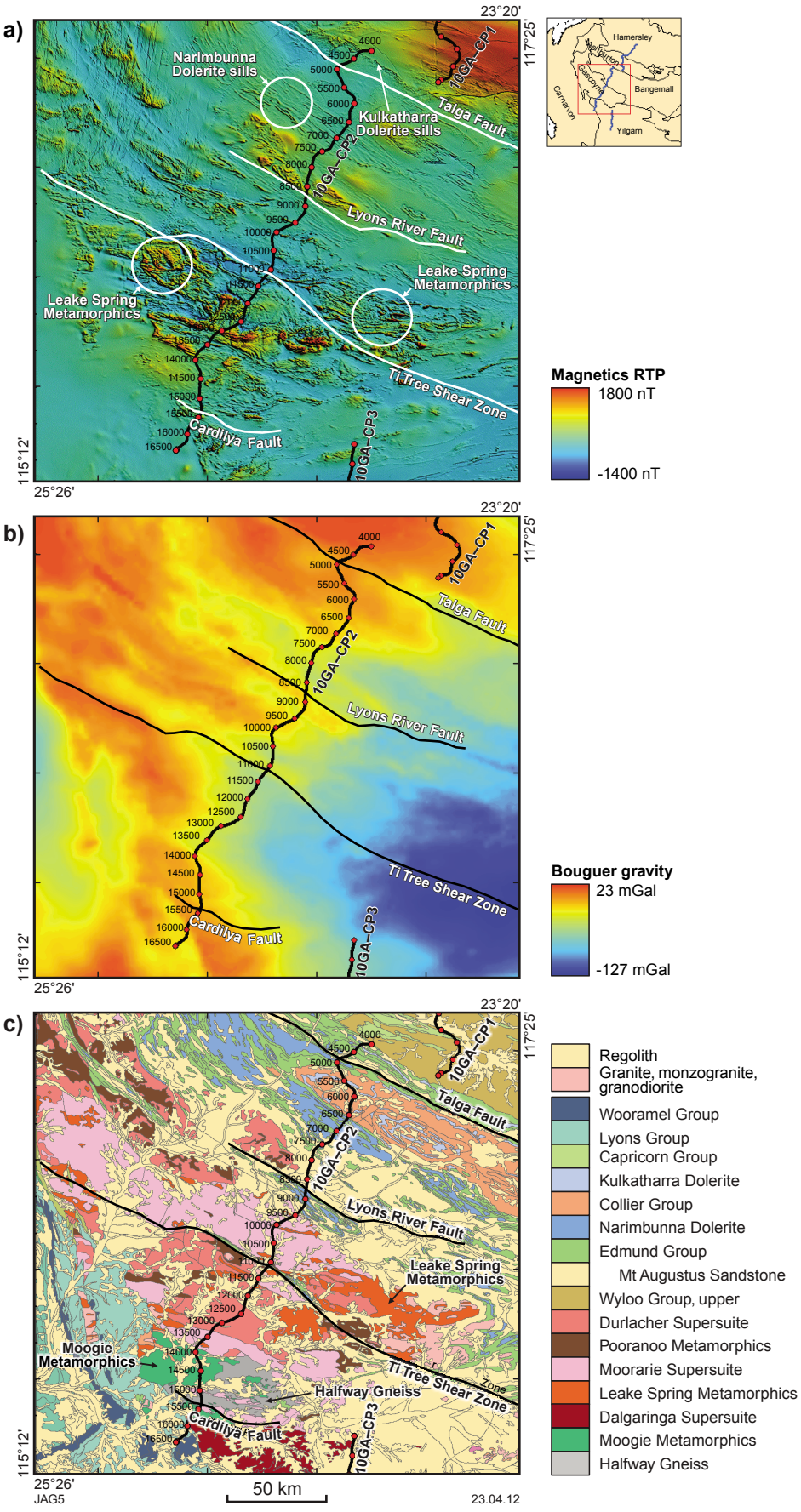

Figure 5. **a) Magnetic grid RTP (with values outside the 98th percentile removed, and sun shading from the northeast applied to highlight contrast in the data); b) bouguer gravity grid; c) 1:1 000 000 scale surface geology map covering seismic line 10GA–CP2.**

extending from the northwest, which splay out into fingers across seismic line 10GA–CP2, before grading into a regional gravity low in the southeast (Fig. 5b).

Three magnetic worms defining southwest-dipping contacts have been identified between CDPs 8600 to 9000, CDPs 11600 to 12000, and CDPs 14700 to 14900 (Fig. 6a). These contacts coincide with the Lyons River Fault, an unnamed fault, and the Cardilya Fault, respectively (Johnson et al., 2011), and suggest that these faults separate areas of contrasting magnetic susceptibility. In particular, the Lyons River and Cardilya Faults are suggested by Johnson et al. (2011) to be major sutures. Gravity worms, on the other hand, define a northeast-dipping contact between CDPs 7000 to 7500 (Fig. 6b), contradictory to the dominant southwest direction of faulting in this area, and perhaps related to a property contrast within or below the shallowly northwest-dipping layers of the Edmund Group.

The magnetic inversion defines a zone of relatively high magnetic susceptibility (0.04 – 0.07 SI) between CDPs 4000 and 10500, which correlates well with the interpreted extent of the Bandee Seismic Province (Fig. 7a). This zone also defines a south-dipping contact consistent with the Lyons River Fault, suggesting that this fault separates two areas of significantly different magnetic susceptibility. In the density inversion, four distinct low-density areas have been modelled at the surface, corresponding approximately with CDPs 8300, 9400, 10800, and 11500 (Fig. 7b). These areas correlate well with outcrops of granite and of the Mount Augustus Sandstone (Fig. 5c). A high density (≥0.05 g/cm^3), near-surface body located at CDPs 9000 is bound by the Lyons River Fault, and correlates well with the interpreted northernmost extent of the Glenburgh Terrane, as identified by Johnson et al. (2011).

Two forward models have been generated for seismic line 10GA–CP2; the first has geometries matched to the seismic interpretation from Johnson et al. (2011; Fig. 8a), and the second is a modified version, where extra detail has been added to produce a better fit with anomalies in the potential-field data (Fig. 8b).

The gravity profile of seismic line 10GA–CP2 peaks in the north with a high of −10 mGal (Fig. 8). Towards the centre of the line, a regional gravity low of −45 mGal is observed, and several short-wavelength, low-amplitude anomalies also occur, coinciding with granites of the Durlacher and Moorarie Supersuites (Fig. 8a,b). Areas where the Mount Augustus Sandstone outcrops also coincide with short-wavelength, low-amplitude gravity anomalies at CDPs 8300 and 9400 (Fig. 8b). Towards the southern end of the seismic line, another peak, of −20.5 mGal, occurs in the gravity data and has a broad-wavelength anomaly. This anomaly has been accounted for in the forward model by attributing densities of 2.78–2.80 g/cm^3 to the Glenburgh Terrane.

To increase the accuracy of the obtained models, a number of extra details were added to the interpretation provided by Johnson et al. (2011), including: the addition of dolerite sills within the Edmund Group to account for short-wavelength gravity and magnetic anomalies; the addition of the Leake Spring Metamorphics to account for short-wavelength, high-amplitude magnetic anomalies, particularly in the southern part of the seismic line; and the separation of the Moogie Metamorphics from the rest of the Glenburgh Terrane to account for the broad-wavelength gravity high (of −20.5 mGal) observed at the southern end of the seismic line (Fig. 8b).

Seismic line 10GA–CP3

The Dalgaringa Supersuite outcrops at the northern end of seismic line 10GA–CP3, and correlates with a smooth-textured region of magnetically low character that is overprinted by northeast-trending, short-wavelength anomalies at CDPs 6000–7500 (Fig. 9a,c). A similar magnetic character is seen at CDPs 7500–8000, although a northeast-trending gravity low is also observed in this area, corresponding with the extent of the Errabiddy Shear Zone (Fig. 9b). Beyond CDP 8000, the seismic line progresses into the Narryer Terrane, which is dominated by short-wavelength magnetic anomalies bearing a stippled texture. These magnetic anomalies correlate well with outcrops of the unit identified by the 1:1 000 000 scale Surface Geology Map of Australia as 'Banded Iron Formation 74257' (Raymond and Retter, 2010), which together form a regional fold, the hinge zone of which lies to the east of seismic line 10GA–CP3 (Fig. 9c).

The magnetic worms covering seismic line 10GA–CP3 delineate a major trend between CDPs 8000 and 9000, which at shallow upward continuation levels of 1400–5379 m, define a steeply north-dipping contact, before transitioning into a south-dipping contact at upward continuation levels of 7531–56 703 m (Fig. 10a). The position of these worms agree well with the northernmost extent of the Narryer Terrane as observed in the surface geology (Fig. 9a), and with the dip direction of faults in the seismic interpretation (Johnson et al., 2011). The gravity worms delineate another major trend at CDPs 6000, ranging from upward continuation levels of 1400–56 703 m, defining a steeply dipping undulating contact, possibly related to the Cardilya Fault (Fig. 10b).

The major feature observed in the magnetic inversion covering seismic line 10GA–CP3 is a high susceptibility (0.04 – 0.07 SI) body originating at the surface at CDP 8000, whose northern margin is south-dipping (Fig. 11a). This body coincides with the northern extent of the Narryer Terrane at the surface (Fig. 9c), and supports the interpretation of major south-dipping faults in the seismic data (Johnson et al., 2011). In particular, the high susceptibility body matches well with the dip direction of an unnamed fault, labelled 'Fault 1' in Figure 11. The gravity inversion also shows the Errabiddy Shear Zone, located between CDPs 7500 and 8000, as a low density (≤–0.05 g/cm^3) feature (Fig. 11b).

Following the interpretation of Johnson et al., (2011), an initial forward model was created for seismic line 10GA–CP3 (Fig. 12a). The initial interpretation separates part of the Dalgaringa Supersuite into sections, with density ranging from 2.60 – 2.75 g/cm^3, to account for the broad-wavelength gravity high of −52.2 mGal seen

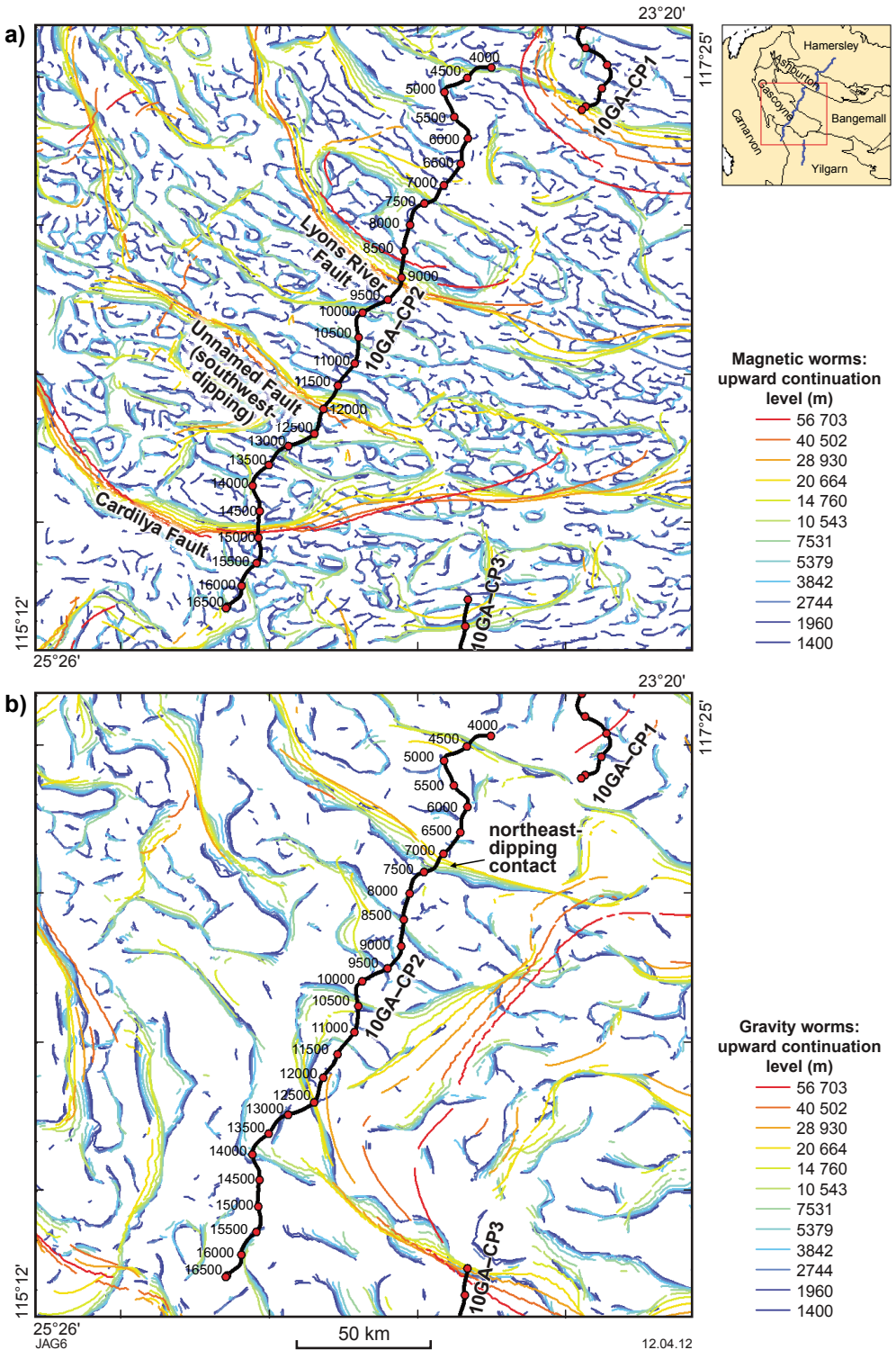

Figure 6. Worm images, covering seismic line 10GA–CP2, for magnetic (a) and gravity (b) data.

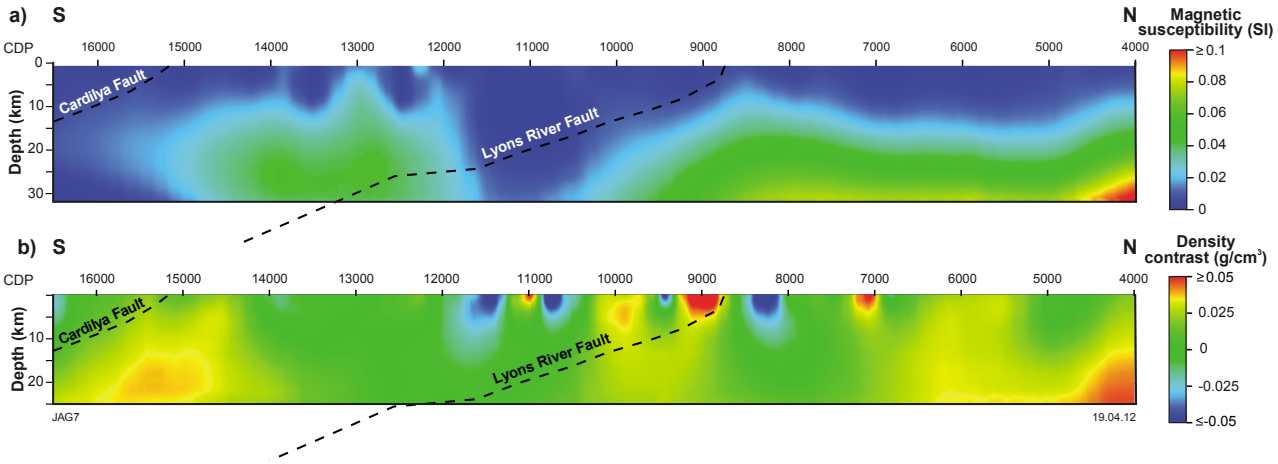

Figure 7. Inversion models extracted along seismic line 10GA–CP2: a) magnetic susceptibility model; b) density model.

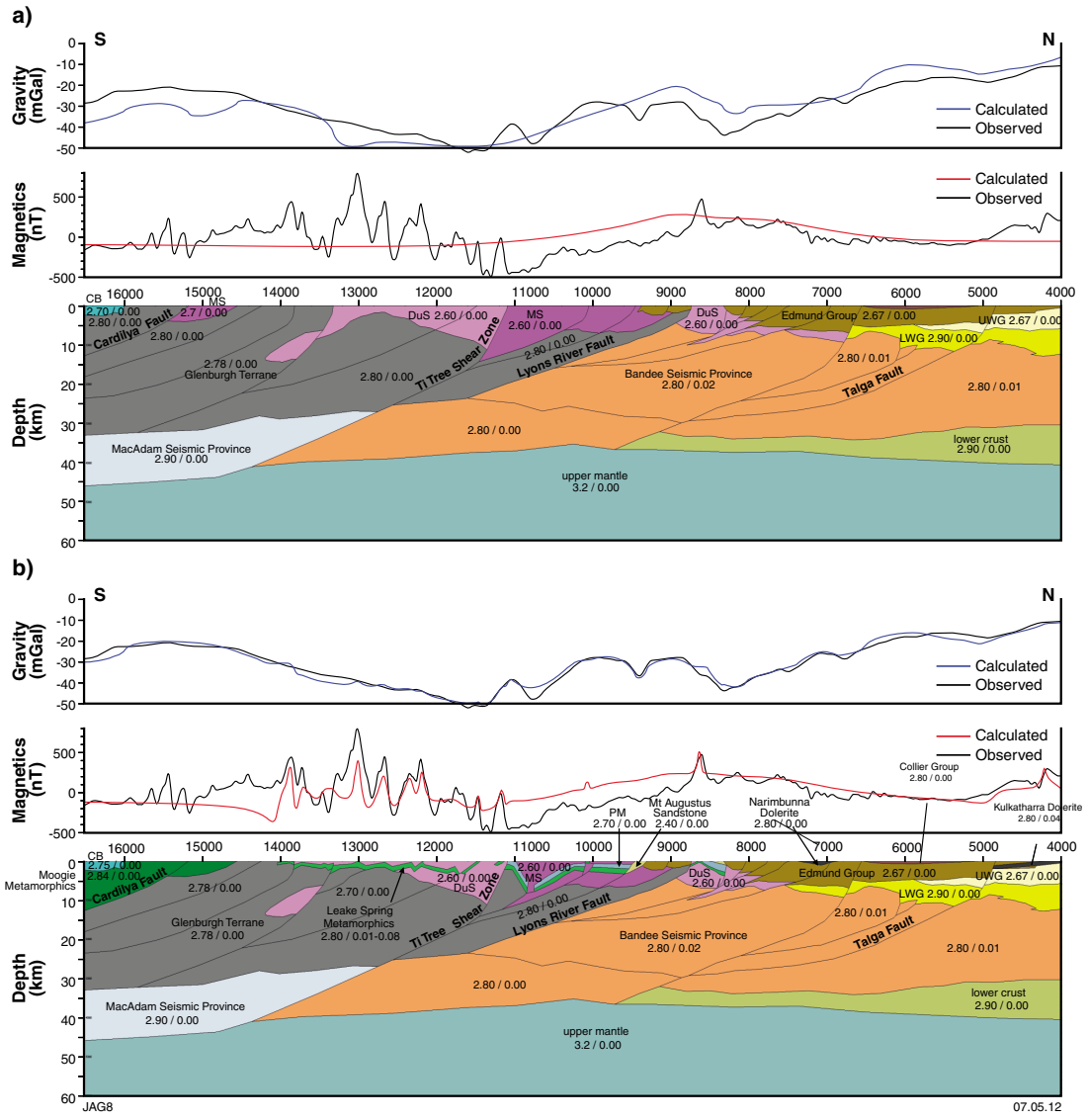

Figure 8. Forward models for seismic line 10GA–CP2: a) initial interpretation using geometries described by Johnson et al. (2011); and b) modified version of (a), altered to produce a better fit with the potential-field data. Rock property values are listed on the figure as density (g/cm³) / magnetic susceptibility (SI). Abbreviations used: PM — Pooranoo Metamorphics; MS — Moorarie Supersuite; DuS — Durlacher Supersuite; UWG — upper Wyloo Group; LWG — lower Wyloo Group; CB — Carnarvon Basin.

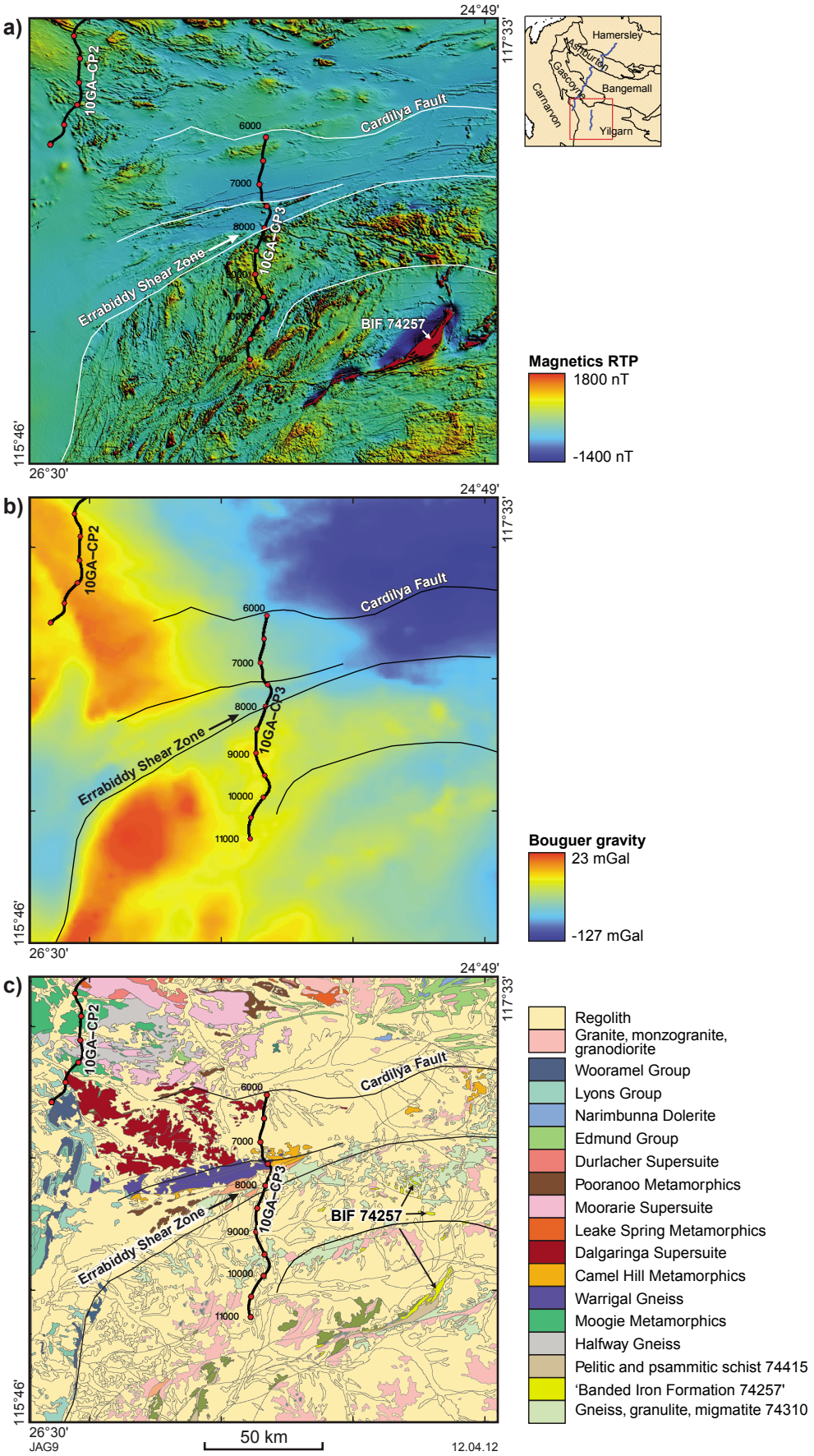

Figure 9. **a) Magnetic grid RTP (with values outside the 98th percentile removed, and sun shading from the northeast applied to highlight contrast in the data); b) bouguer gravity grid; c) 1:1 000 000 scale surface geology map covering seismic line 10GA–CP3.**

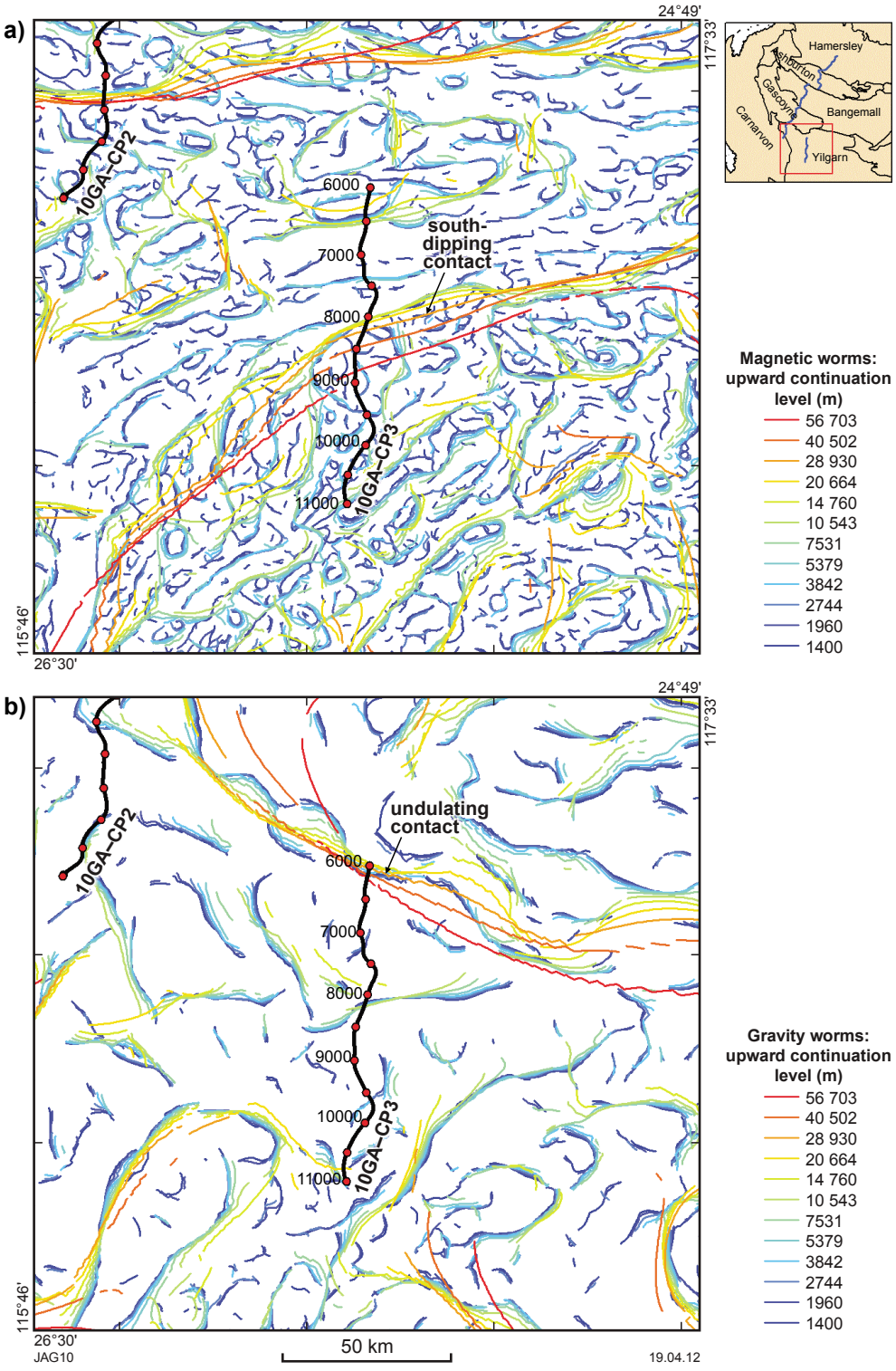

Figure 10. Worm images, covering seismic line 10GA–CP3, for magnetic (a) and gravity (b) data.

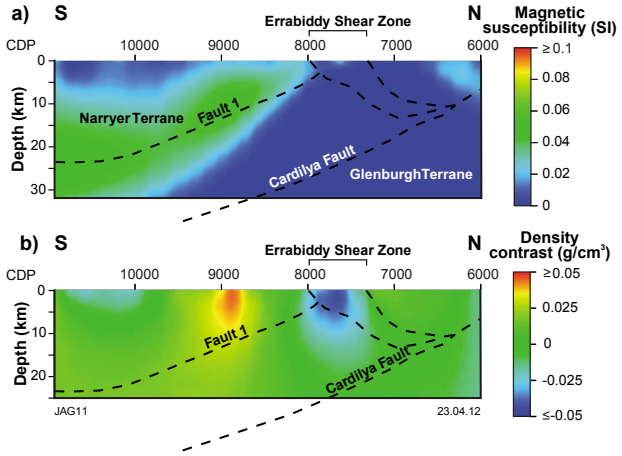

Figure 11. Inversion models extracted along seismic line 10GA–CP3: a) magnetic susceptibility model; b) density model.

at the northern end of the seismic line. Another possibility is shown in the modified interpretation, which accounts for this same gravity feature by placing a denser body of Moogie Metamorphics (2.90 g/cm^3) beneath the Dalgaringa Supersuite (Fig. 12b). The extent of this dense body of Moogie Metamorphics matches form lines observed in the seismic interpretation (Johnson et al., 2011).

In the initial forward model, the Narryer Terrane varies in density from 2.70 – 2.80 g/cm^3 to account for the gravity peak of −32.4 mGal, and in magnetic susceptibility from 0.00 – 0.02 SI to account for the relatively higher magnetic responses observed in the south of the study area (Fig. 12a). As part of the Narryer Terrane was modelled in the initial interpretation as being of low magnetic susceptibility, this section has been separated from the rest of the Narryer Terrane, forming a middle crust layer (0.00 SI) in the modified interpretation (Fig. 12b). This separation is supported by both the magnetic worms and magnetic inversion, which define a south-dipping body coinciding with ‘Fault 1’. It is also noted that short-wavelength, high-amplitude magnetic anomalies across the Narryer Terrane are not accounted for in the initial interpretation, and have been modelled using the 500 m thick, south-dipping beds of ‘Banded Iron Formation 74257’ (0.015 – 0.070 SI; Fig. 12b), based on the correlation of this unit with the magnetic anomalies mentioned above (see Fig. 9).

Conclusion

Using multiscale edge detection, 3D inversion, and 2.5D forward modelling, a number of geophysical terranes, contrasting properties, and major trends have been identified in the gravity and magnetic data covering the area of Capricorn Orogen seismic lines. The major sources of magnetic anomalies observed throughout the Capricorn

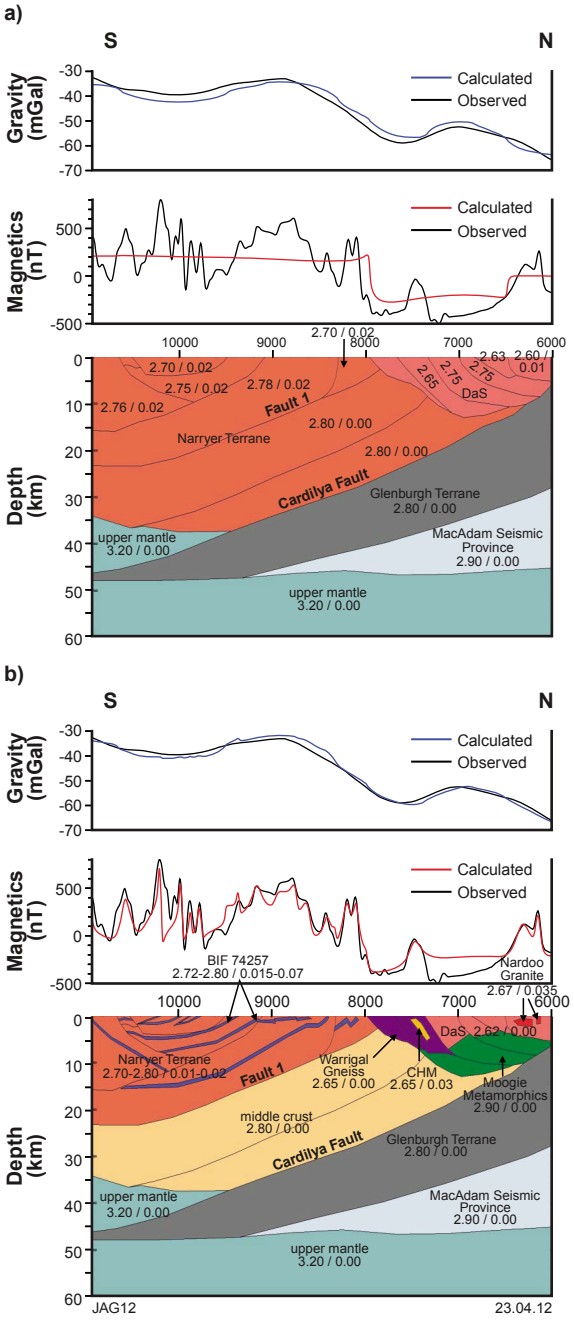

Figure 12. Forward models for seismic line 10GA–CP3: a) initial interpretation using geometries described by Johnson et al. (2011); and b) modified version of (a), altered to account for details observed in the potential-field data. Rock property values are listed on the figure as density (g/cm^3) / magnetic susceptibility (SI). Abbreviations used: CHM — Camel Hills Metamorphics; BIF — Banded Iron Formation; DaS — Dalgaringa Supersuite.

Orogen are attributed to the Hamersley Group, Bandee Seismic Province, Leake Spring Metamorphics, 'Banded Iron Formation 74257', and the Narryer Terrane.

Forward models generated using the geometries interpreted from the Capricorn seismic lines have indicated that these geometries can be modelled, using reasonable rock properties, to achieve a response that matches the observed potential-field data. This result indicates that the seismic interpretation is broadly consistent with the potential-field data. Nevertheless, further detail needed to be assumed for seismic lines 10GA–CP2 and 10GA–CP3, particularly to account for short-wavelength features observed in this potential-field data.

Two sutures identified in the seismic interpretation, the Baring Downs Fault and the Lyons River Fault, coincide with contacts between different magnetic terranes identified in the magnetic worms, 3D inversions, and forward models. A third suture, the Cardilya Fault, agrees with aspects of the gravity and magnetic worms, but does not agree with features identified in the inversions. In addition, an unnamed fault labelled 'Fault 1' (Fig. 12) is shown in the magnetic worms, 3D inversion, and modified forward model to separate a highly magnetic portion of the Narryer Terrane from a non-magnetic middle crust.

Acknowledgements

I would like to thank Richard Chopping, Russell Korsch, Malcolm Nicoll, and Richard Blewett for their assistance and insight. I would also like to thank Tony Meixner, Russell Korsch, and Richard Chopping for reviewing this extended abstract. Published with permission of the Chief Executive Officer, Geoscience Australia.

References

Archibald, NJ, Gow, P and Boschetti, F 1999, Multiscale edge analysis of potential field data: Exploration Geophysics, v. 30, p. 38–44.

Bacchin, M, Milligan, P, Tracey, R and Wynne, P 2008, Gravity Anomaly Map of the Australian Region (3rd edition): Geoscience Australia, Canberra, Australian Capital Territory, 1:5 000 000 scale map.

Beardsmore, GR and Cull, JP 2001, Crustal heat flow: a guide to measurement and modelling: Cambridge University Press, Cambridge, UK, 324p.

Cawood, PA and Tyler, IM 2004, Assembling and reactivating the Proterozoic Capricorn Orogen: lithotectonic elements, orogenies, and significance: Precambrian Research, v. 128, p. 201–218.

Clark, DA and Emerson, DW 1991, Notes on rock magnetization characteristics in applied geophysical studies: Exploration Geophysics, v. 22, p. 547–555.

Cull, JP and Denham, D 1979, Regional variations in Australian heat flow: BMR Journal of Australian Geology and Geophysics, v. 4, p. 1–13.

Cutten, HN, Thorne, AM and Johnson, SP 2011, Geology of the Edmund and Collier Groups, *in* Capricorn Orogen seismic and magnetotelluric (MT) workshop 2011: extended abstracts *edited by* SP Johnson, AM Thorne and IM Tyler: Geological Survey of Western Australia, Record 2011/25, p. 41–48.

Emerson, DW 1990, Notes on mass properties of rocks — density, porosity, permeability: Exploration Geophysics, v. 21, p. 209–216.

Guo, WW, Li, ZX and Dentith, MC 2011, Magnetic petrophysical results from the Hamersley Basin and their implications for interpretation of magnetic surveys: Australian Journal of Earth Sciences, v. 58, p. 317–333.

Holden, DJ, Archibald, NJ, Boschetti, F and Jessell, MW 2000, Inferring geological structures using wavelet-based multiscale edge analysis and forward models: Exploration Geophysics:, v. 31, p. 617–621.

Johnson, SP, Cutten, HN, Tyler, IM, Korsch, RJ, Thorne, AM, Blay, O, Kennett, BLN, Blewett, RS, Joly, A, Dentith, MC, Aitken, ARA, Goodwin, JA, Salmon, M, Reading, A, Boren, G, Ross, J, Costelloe, RD and Fomin, T 2011, Preliminary interpretation of deep seismic reflection lines 10GA–CP2 and 10GA–CP3: crustal architecture of the Gascoyne Province, and Edmund and Collier Basins, *in* Capricorn Orogen seismic and magnetotelluric (MT) workshop 2011: extended abstracts *edited by* SP Kohnson, AM Thorne and IM Tyler: Geological Survey of Western Australia, Record 2011/25, p. 49–60.

Kennett, BLN, Tyler, IM, Maher, J, Holzschuh, J, Fomin, T and Costelloe, RD 2011, The Capricorn seismic survey: experimental design, acquisition, and processing, *in* Capricorn Orogen seismic and magnetotelluric (MT) workshop 2011: extended abstracts *edited by* SP Johnson, AM Thorne and IM Tyler: Geological Survey of Western Australia, Record 2011/25, p. 1–6.

Li, Y and Oldenburg, DW 1996, 3-D inversion of magnetic data: Geophysics, v. 61, p. 394–408.

Li, Y and Oldenburg, DW 1998, 3-D inversion of gravity data: Geophysics, v. 63, p. 109–119.

Milligan, PR, Franklin, R, Minty, BRS, Richardson, LM and Percival, PJ 2010, Magnetic Anomaly Map of Australia (5th edition): Geoscience Australia, Canberra, Australian Capital Territory, 1:5 000 000 scale map.

Raymond, OL and Retter, AJ (editors) 2010, Surface geology of Australia, 2010 edition: Geoscience Australia, Commonwealth of Australia, Canberra, Australian Capital Territory, <http://www.ga.gov.au>, 1:1 000 000 scale digital dataset.

Sheppard, S, Rasmussen, B, Muhling, JR, Farrell, TR and Fletcher, IR 2007, Grenvillian-aged orogenesis in the Palaeoproterozoic Gascoyne Complex, Western Australia: 1030–950 Ma reworking of the Proterozoic Capricorn Orogen: Journal of Metamorphic Geology, v. 25, p. 477–494.

Telford, WM, Geldart, LP, Sheriff, RE and Sheriff, RE 1990, Applied geophysics: Cambridge University Press, Cambridge, UK, 792p.

Thorne, AM, Tyler, IM, Korsch, RJ, Johnson, SP, Brett, JW, Cutten, HN, Blay, O, Kennett, BLN, Blewett, RS, Joly, A, Dentith, MC, Aitken, ARA, Holzschuh, J, Goodwin, JA, Salmon, M, Reading, A and Boren, G 2011, Preliminary interpretation of deep seismic reflection line 10GA–CP1: crustal architecture of the northern Capricorn Orogen, *in* Capricorn Orogen seismic and magnetotelluric (MT) workshop 2011: extended abstracts *edited by* SP Johnson, AM Thorne and IM Tyler: Geological Survey of Western Australia, Record 2011/25, p. 19–26.